

Atlas of Main-line OH Masers in the Galactic Longitude Range 3° to 60°

J. L. Caswell and R. F. Haynes

Division of Radiophysics, CSIRO,
P.O. Box 76, Epping, N.S.W. 2121.

Abstract

We tabulate all 55 OH main-line masers discovered to date in the galactic plane between longitude 3° and 60° . For most of these we show current spectra, which have been taken with the Parkes 64 m radio telescope, in both senses of circular polarization on the 1665 MHz and/or 1667 MHz transitions; for some sources we give new position estimates, and several sources are reported for the first time. We discuss many sources individually and note that while most of the main-line OH masers probably pinpoint compact HII regions and sites of current star formation, a few appear to be unusual varieties occurring in circumstellar shells, possibly associated with late-type stars.

The 55 sources are approximately half as many as those found in the Parkes survey of the complementary southern region; this reflects the lower sensitivity and less uniform coverage of the northern surveys on which the present atlas is largely based and precludes its use in the study of the galactic distribution of OH masers. However, following our present measurements, the sources have become a valuable addition to the sample for studying associations with HII regions and H₂O masers, polarization and velocity structure, relative line intensities and variability.

1. Introduction

In the decade following the discovery of OH maser emission, effort was largely concentrated on searching for emission from specific astronomical objects such as HII regions, late-type stars and planetary nebulae.

In the case of main-line OH masers, which are commonly associated with sites of star formation and young HII regions, *systematic surveys* have now been made with the Parkes 64 m telescope (beamsize $12'$ arc at 18 cm wavelength) over the longitude range $300^\circ \rightarrow 360^\circ \rightarrow 2^\circ$ along the galactic plane ($b \approx \pm 0^\circ \cdot 3$, with wider coverage where the radio continuum emission indicates much greater thickness of the plane). The surveys extend to masers slightly weaker than 1 Jy ($\equiv 10^{-26} \text{ W m}^{-2} \text{ Hz}^{-1}$), and most masers have been positioned with r.m.s. uncertainties of $< 30''$.

Much of the northern region, $l > 2^\circ$, was included in Turner's (1979) OH survey with the NRAO 42 m telescope (beamsize $18'$ arc). Turner did not observe at a uniform grid of positions and the survey is most useful for the study of absorption rather than emission. Compared with the Parkes survey the sensitivity is poorer for emission from point sources with small velocity width and high circular polarization. Moreover, Turner made no attempt to position sources, with the result that in many cases multiple entries in his list refer to a single source detected at different telescope positions. Some of the masers in the northern region were known from earlier searches at the position of HII regions while others are seen for the first time in Turner's data.

To make the northern survey useful for the study of main-line OH masers we have attempted to re-observe all the reported sources in the longitude range $2^\circ \rightarrow 60^\circ$, to measure each position and to obtain a high-resolution spectrum in each sense of circular polarization. We failed to detect a few of the weaker sources; these may be outside the search area that we covered, or they may show variability, or they may represent extended quasi-thermal emission (and show a weaker signal on our smaller beam), or some may be spurious. However, most sources were detected satisfactorily, and we have compiled a catalogue of all known main-line OH masers in the region, together with positions and profiles comparable with those of masers in the more completely observed southern sky. Some of our listed sources were not seen on the Turner (1979) profiles, and our detections of them have a variety of origins, usually a result of studying independently discovered H₂O masers or complex HII regions.

2. Results

The results were obtained in the same series of observations as our southern survey of the OH ground-state main lines at 1665 and 1667 MHz (Caswell *et al.* 1980; Caswell and Haynes 1983, present issue p. 361). In our previous surveys rest frequencies of 1665.401 and 1667.358 MHz were assumed; in this paper we adopt the revised values of 1665.402 and 1667.359 MHz (ter Meulen and Dymanus 1972). We used a dual-channel parametric amplifier installed on the Parkes 64 m paraboloid to obtain 512-point spectra for each circular polarization simultaneously. The intensity calibration is relative to Hydra A, which has a total flux density of 36 Jy (i.e. 18 Jy in each sense of circular polarization; the ratio of flux density to antenna temperature for each polarization is 0.8 Jy K^{-1}). The beamwidth to half-power is $12'$ arc at 1666 MHz. Where new position estimates were needed, these were obtained from observations at a grid of points spaced $12'$ in both right ascension and declination; for the stronger sources, residual r.m.s. errors are typically $15''$ arc in each coordinate. Final on-source spectra were usually obtained with 0.2 MHz total bandwidth, to yield, after Hanning-weighting, a resolution of 0.8 kHz (0.14 km s^{-1}). Table 1 summarizes the results; it lists the OH main-line masers with peak intensity of $> 1 \text{ Jy}$ located in the longitude range 3° to 60° and is believed to contain all the sources discovered as of 1982 February; it excludes objects which have the *unambiguous* characteristics of late-type stars, in which 1612 MHz emission dominates and 1667 or 1665 MHz emission is present at much lower levels. The positions (columns 1, 2 and 3) are taken from either our own measurements or from an italicized reference in column 10. The range of radial velocity over which emission is seen is given in column 5. Columns 6, 7, 8 and 9 list the peak intensity on each of the ground-state transitions; the sense of circular polarization with strongest emission is indicated and the transition used for position measurements is italicized. Our new measurements (see also Figs 1–12) were used for most of the main-line data while upper limits on satellite-line emission are mostly from Turner (1979) and are expressed in fractions of the main-line intensity as measured by Turner; this partly overcomes the problem that Turner's profiles are not usually at the precise source position and are of lower velocity resolution than our main-line measurements. References in column 10 are to figure numbers (showing current spectra), to position measurements, and to earlier spectra suitable for variability comparisons.

The presence of nearby H₂O emission is noted in column 11. Radio continuum and recombination-line data are summarized in column 12 and are discussed more

fully in the notes of Section 3. The kinematic distance estimate to the source is given in column 13; it is based on the Schmidt (1965) galactic rotation model with an assumed distance of Sun to galactic centre of 10 kpc, and where there is evidence strongly favouring either the near or far distance the less probable distance is given in parentheses.

Our spectra at 1665 and 1667 MHz were taken for most of the sources in 1982 February and are shown in Figs 1–12. In the following discussion of individual sources frequent comparisons are made with the 5 GHz continuum and recombination-line data of Haynes *et al.* (1978), Altenhoff *et al.* (1978) and Downes *et al.* (1980).

3. Notes on Some Individual OH Sources

OH 3.91–0.01 (Fig. 1). A single feature, 100% right-hand circularly polarized, is seen at 1665 MHz and nothing at 1667 MHz or the satellite lines. No discrete continuum source is present.

OH 5.88–0.39. This unusual source shows 1665 and 1667 MHz maser emission over the large velocity range -44 to $+17$ km s⁻¹, and a strong 1612 MHz maser at $v = -21$ km s⁻¹. Our unpublished data show that (i) the 1667 and 1665 MHz spectra in 1976 August had changed little since 1968 when Turner's (1969) spectra were recorded [but note that our observations reveal an error in Turner's data in both table and figure, with the line velocities wrong by ~ 10 km s⁻¹; the correct velocities are seen in Turner (1979)]; (ii) the 1612 MHz line had decreased in intensity from a peak of 80 Jy in each polarization in 1968 to 23 Jy by 1978 August. Although we have no recent spectra, several lines of evidence prompt us to reassess the current classification of this object. The maser was interpreted as circumstellar emission from a late-type star by Baud *et al.* (1979), principally on the basis of their discovery of weak 1612 MHz emission at $v = +13$ km s⁻¹; this they assumed to be associated with the strong 1612 MHz emission at $v = -21$ km s⁻¹, and thus to indicate the double-peaked velocity structure at 1612 MHz characteristic of such stars. However, we note that Turner's (1979) spectrum of the 1720 MHz transition in this direction shows *absorption* near $v = +13$ km s⁻¹, precisely matching in velocity the weak 1612 MHz emission shown by Baud *et al.*; the intensities of the 1612 and the 1720 MHz features (measured with the NRAO 140 foot telescope) are very similar in magnitude ($T_a \approx 0.3$ K) but opposite in sign, and this is typical of Type IIc OH emission (Caswell and Haynes 1975) which arises in *extended* molecular clouds. On this interpretation we note that the molecular cloud is probably loosely associated with the quite strong HII region in this direction, which has a recombination-line velocity centred at $+9$ km s⁻¹.

What then is the classification of the bulk of the OH emission? The velocity structure at 1665 and 1667 MHz is suggestive of an expanding (or contracting) shell and *might* represent emission from a late-type star, but several other properties are atypical of such sources: (i) the 1612 MHz emission lies *within* the range of main-line velocities rather than outside it; (ii) there is associated H₂O emission in the velocity range $+7$ to $+20$ km s⁻¹, but it arises from *two* regions, separated by $18''$ arc (Genzel and Downes 1977), whereas in late-type stars the emission is confined to a circumstellar envelope of <0.01 pc (e.g. $1''$ arc at a distance of 2 kpc); (iii) the associated H₂O maser has high-velocity features at -61 and $+86$ km s⁻¹, such features being characteristic of the H₂O masers in star-formation regions and not of late-type stars.

Table 1. OH main-line masers in galactic plane between longitudes 3° and 60°

(1) Galactic coordinates <i>l</i> °	(2) Position (1950) R.A. h m s	(3) Dec. ° ' "	(4) r.m.s. error "	(5) Radial velocity ^A (km s ⁻¹)	(6) 1665 (Jy)	(7) Intensity (polarization) of peak ^B (Jy)	(8) 1612 (Jy)	(9) 1720 (Jy)	(10) OH refs ^C	(11) H ₂ O?	(12) Radio continuum	(13) Kinematic distance ^D (kpc)
3-91-0-01	17 51 35.6	-25 34 19	18	+18	4-6(R)	<0.3	<1665/5	<1665/5	Fig. 1	Y	Weak plateau (0.3 Jy)	5.8, 14.2
5-88-0-39	17 57 26.7	-24 04 01	10	-44, +17	~4	~18	~23	<1667/100	H; WTM; T69	Y	Strong HII, $v = 10.5$	—
8-68-0-37	18 03 24.1	-21 37 34	21	+35, +42	3-7(L)	2-4(L)	<1665/5	<1665/5	Fig. 1	Y	Compact HII, $v = 40$	5.8, 14
9-62+0-19	18 03 17.6	-20 31 54	15	-2, +23	7-9.2(L)	17(L)	<1665/3	<1665/2	Fig. 1	Y	HII, $v = 3$	—
10-62-0-38	18 07 30.4	-19 56 28	2	-3, +1	30(R)	18-5(R)	<1665/6	≤1665/6	Fig. 3; CR; T82	Y	Strong HII, $v = 0$	See text
11-03+0-06	18 06 43.3	-19 22 01	17	+20, +23	7-2(R)	<1665/16	<1665/16	~1665/4?	Fig. 3	Y	Compact continuum	3.2, 16
11-91-0-15	18 09 18.1	-18 42 25	16	+39, +43	6-6(L)	1-7(L)	<1665/6	<1665/4	Fig. 3	Y	Edge of HII, $v = 41.5$	5.1, 14.4
12-03-0-04	18 09 07.4	-18 32 39	16	+106, +110	3-7(R)	0-7(R)	?	?	Fig. 3	Y	Nothing?	8.4, 11.2
12-22-0-12	18 09 48.4	-18 25 13	2	+20, +31	21(R)	16(L)	<1665/40	<1665/40	Fig. 3; T82	Y	Compact HII, $v = 25$	(3.4), 16.1
12-68-0-18	18 10 59.6	-18 02 47	3	+58, +66	17-3(R, L)	~1665/2.5	<2	<2	Fig. 3; W/W'; RGM	Y	Complex HII	6.4, (13.1)
12-91-0-26	18 11 44.3	-17 52 57	3	+28, +42	95(L)	44(L)	<2	<2	Fig. 4; W/W'; E	Y	Strong HII	4.4, (15.1)
14-17-0-06	18 13 32.3	-16 40 53	21	+29, +61	1-4(R)	7-4(R)	<1667/3	<1667/3	Fig. 4	Y	Complex HII	5.0, 14.4
15-04-0-68	18 17 31.9	-16 12 51	Note ^E	+21, +23	2-0(R, L)	<0.5	<1665/10	<1665/10	HCG	Y	M 17, $v = 17$	2.5, (16.7)
16-59-0-06	18 18 20.3	-14 33 18	16	+58, +63	4-7(R)	<1665/10	<1665/10	<1665/10	Fig. 4	Y	0.1 Jy continuum	5.6, 13.6
18-46-0-01	18 21 48.0	-12 53 02	16	+32, +55	2-9(R)	1-5(R)	<1665/5	<1665/5	Fig. 5	Y	Compact continuum	4.1, 14.9
19-48+0-16	18 23 10.3	-11 54 31	22	+13, +26	3-7(R)	4-4(R)	~1667/2	<1667/2	Fig. 5	Y	Ext. HII, $v = 25$	1.9, 16.9
19-61-0-23	18 24 49.9	-11 58 31	5	+40, +43	3-8(R)	~1665/6	<1665/10	≤1665/7	Fig. 5; G	Y	HII; $v = 43$	4.3, (14.6)
20-08-0-13	18 25 22.7	-11 30 47	6	+42, +50	11-7(L)	~1665/15	<1665/10	<1665/10	Fig. 5; G	Y	Compact HII; $v = 46$	4.1, (14.7)
20-24+0-08	18 24 55.8	-11 16 24	20	+72, +78	1-7(R)	<1665/4	<1665/5	<1665/10	Fig. 5	Y	Nothing?	6.0, 12.7
20-86+0-48	18 24 39.8	-10 32 18	10	+35, +65	2-0(R, L)	~1665/5	2.6 × 1665	<1665/10	WTM	Y	Nothing	4.4, 14.3
22-44-0-18	18 30 01.0	-09 27 00	19	+24, +35	4-8(R)	≤0.7(L)	<1665/5	<1665/5	Fig. 6	Y	See text	2.7, 15.8
23-01-0-41	18 31 56.7	-09 03 18	15	+65, +80	4-9(R)	1-4(R)	<1665/3	<1665/3	Fig. 6	Y	Edge of diffuse HII	(5.6), 12.8
23-43-0-19	18 31 55.8	-08 34 17	20	+103, +108	4-7(R)	0-6(R)	<1665/3	<1665/5	Fig. 6	Y	Strong HII, $v = 104$	7.8, 10.5
24-33+0-11	18 32 3.3	-07 38 24	5	+62, +87	~1667/10	<1667/10	<1667/10	<1667/10	Fig. 6; G	Y	See text	5.6, 12.6
24-78+0-08	18 33 30.6	-07 15 07	20	+100, +110	5-5(R)	<1665/10	<1665/5	<1665/5	Fig. 6	Y	Near HII, $v = 113$	7.7, 10.4
27-35-0-20	18 39 16.0	-05 06 35	45	+79, +88	1-7(R)	≤0.4	<1665/2	<1665/2	Fig. 7	Y	Diffuse HII, $v = 98$	6.0, 11.7
28-21-0-05	18 40 21.6	-04 16 26	20	+92, +103	15-0(R)	3-0(R)	<1665/40	<1665/40	Fig. 7	Y	Compact continuum	6.9, 10.7
28-83-0-25	18 42 12.4	-03 49 08	16	+78, +94	4-2(R)	1-0(R)	≤1665/2	<1665/6	Fig. 7	Y	HII, $v = 92$	6.3, 11.2
28-87+0-06	18 41 10.2	-03 38 36	16	+102, +109	11-3(L)	3-3(L)	≤1665/3	≤1665/3	Fig. 8	Y	Weak continuum	8.5
30-22-0-15	18 44 24.0	-02 32 00	60	+107, +109	1-0(L)	0.7(L)	≤1665/2	≤1665/2	Fig. 8	Y	HII, $v = 101$	8.5

30-39-0-70	18 46 42-0	-02 38 14	11	+48, +64	2-5(R)	≤ 0-6	~ 3 × 1665	< 1665/14	Fig. 8; WTM	None?	3-9, 13-3
30-60-0-06	18 44 45-0	-02 09 15	35	+35, +41	7-0(L)	6-6(L)	≤ 1665/10	< 1665/20	Fig. 8; RGM	In W43 complex	2-8, 14-4
30-70-0-06	18 44 58-9	-02 04 27	30	+85, +105	19(R)	12(R)			Fig. 9	In W43 complex	7-4, 9-8
30-79-0-06	18 45 08-8	-01 59 12	30	+102, +116	2-0(R)	2-5(L)			Fig. 9	In W43 complex	8-5
30-82+0-28	18 44 00-5	-01 48 29	35	+99, +105	3-4(R)	1-0(R)	< 1665/4	< 1665/14	Fig. 9	Weak, within W43	8-5
31-21-0-18	18 46 20-9	-01 40 13	12	-31, -29	~1(R, L)	< 1665/4			WTM	See text	—
31-24-0-11	18 46 10-4	-01 36 41	17	+20, +23	5-3(L)	< 0-5	< 1665/10	< 1665/10	Fig. 10	Weak, towards W43	1-6, 15-5
31-29+0-06	18 45 38-6	-00 19 26	30	+103, +109	2-5(L)	1-0(L)	< 1665/10	< 1665/10	Fig. 10	Compact, in W43	8-5
32-74-0-07	18 48 46-0	-00 15 28	35	+25, +41	2-5(L)	1-1(L)	< 1665/10	< 1665/10	Fig. 10	SNR?	2-5, 14-3
33-13-0-09	18 49 33-6	+00 04 25	11	+72, +82	8-2(L)	3-2(R)	< 1665/5	< 1665/5	Fig. 10; WTM	HII, $\nu = +97$	5-6, 11-1
34-26+0-15	18 50 46-1	+01 11 12	2	+54, +63	55(R)	88(L)	< 1665/10	< 1665/10	Fig. 11; T82	Strong HII, $\nu = 54$	4-2, (12-3)
35-03+0-35	18 51 30-3	+01 57 30	16	+40, +49	8-1(R)	1-9(L)	< 1665/15	< 1665/15	Fig. 11	Compact continuum	3-0, 13-3
35-19-0-74	18 55 40-0	+01 36 22	25	+28, +38	2-8(R)	0-8(R)			Fig. 11; WTM	See text	2-3, 14-0
35-20-1-73	18 59 12-5	+01 09 16	5	+38, +46	42(L)	14-3(L)	< 1665/20	< 1665/20	Fig. 12; E	Strong HII, $\nu = 46$	2-9, (13-4)
35-58-0-03	18 53 51-7	+02 16 31	5	+47, +52	35(R)	6-6(L)	< 1665/30	< 1665/30	Fig. 12; E	Strong HII, $\nu = 51$	13-5, (12-8)
40-62-0-14	19 03 34-9	+06 41 55	5	+28, +37	80(L)	19-3(L)	< 1665/25	< 1665/25	Fig. 12; E	Nothing	2-3, 12-9
43-16-0-03	19 07 58-2	+08 59 58	2	+14, +20	~100	~100(L)	~ 15(R)	~ 50(L)	RE	W49S strong HII	(1-1), 13-4
43-17+0-01	19 07 49-9	+09 01 18	2	-33, +31	~150	~1665/20	< 1665/100	< 1665/100	T82; E	W49N strong HII	(0), 14
43-80-0-13	19 09 30-8	+09 30 47	2	+37, +42	90(L)	~1665/5	< 1665/30	< 1665/30	CR; G	Extended HII	2-6, 11-8
45-07+0-13	19 11 00-4	+10 45 44	5	+55, +61	26(R)	≤ 1665/5	< 1665/30	< 1665/30	CR; G	Compact HII	(4-3), 10
45-10+0-12	19 11 06	+10 46 48	15	+52, +55	13(L)	≤ 1665/5	< 1665/30	< 1665/30	CR; G	Edge of HII	(4-0), 10
45-47+0-13	19 11 46-1	+11 07 06	6	+58, +60	25(L)	≤ 1665/6	< 1665/30	< 1665/30	CR; G	Compact HII	(4-7), 9-3
45-47+0-05	19 12 04-4	+11 04 15	5	+64, +69	20(R)	≤ 1665/6	< 1665/30	< 1665/30	CR; G	Compact HII	(5-4), 8-6
48-61+0-02	19 18 13-0	+13 49 46	5	+18, +21	18(L)	~12(L)	< 1665/15	< 1665/15	CR; E	HII	(1-5), 11-8
49-49-0-39	19 21 26-3	+14 24 37	3	+55, +62	93(L)	≤ 1665/10	~ 24(R)	~ 32(R)	N; RE	W51 HII	(5-3), 7-7

A Range of radial velocity (with respect to l.s.r.) showing detectable emission.
 B Transition used for position measurement is italicized. Lower resolution data (mainly from Turner 1979) are quoted as fractions of the main-line intensity at the same lower resolution; for example, < 1665/5 for the 1612 MHz emission indicates that there is no 1612 MHz emission, with an upper limit of one-fifth the intensity of the 1665 MHz emission (measured at low resolution).
 C References: H, Hardebeck (1972); WTM, Winnberg *et al.* (1981); T69, Turner (1982); CR, Caswell and Robinson (1974); WWW, Wynn-Williams *et al.* (1974); RGM, Robinson *et al.* (1970); E, Evans *et al.* (1979); HCG, Haynes *et al.* (1976); G, Goss *et al.* (1973); RE, Raimond and Eliasson (1969); N, Norris *et al.* (1982).
 D Near and far distances are given; where evidence favours one of these the less likely value is given in parentheses.
 E Position quoted is for excited state emission; see note in text.

Vital measurements needed to clarify the nature of this source include more accurate positions for the OH masers and the H₂O masers to ensure that we are dealing with related objects rather than an unlikely chance superposition. The proposed IR counterpart has a K magnitude of ~ 10.9 ; its position (1950) is R.A. $17^{\text{h}} 57^{\text{m}} 26^{\text{s}}.75$, Dec. $-24^{\circ} 04' 03''$ [where we have averaged the values given by Jones *et al.* (1983) and Epchtein and Rieu (1982) on the assumption that they refer to the same object, despite their nominal difference of $16''$ arc]. This position needs refinement and attempts should be made to assess whether it is an early- or late-type object.

Overall we conclude that the evolutionary status of the object giving rise to the maser emission is not clear; on current evidence it cannot be assumed to be a typical circumstellar maser of the OH/IR late-type star variety, and indeed it seems more likely to be a young object in a star-formation region.

OH 8.68-0.37 (Fig. 1). The OH maser, detected at both 1665 and 1667 MHz, is located within $\sim 1'$ arc of a compact HII region with flux density 1.4 Jy and an H₂O maser (Genzel and Downes 1979). Slightly offset in velocity from the OH maser (to $v = +36$ km s⁻¹) there is OH absorption (of 0.6 Jy), indicating a more extensive OH cloud which is probably absorbing both the compact HII region and some of the more diffuse background.

OH 9.62+0.19 (Fig. 1). Both 1665 and 1667 MHz profiles show emission in the two velocity ranges -2 to $+7$ km s⁻¹ and $+20$ to $+23$ km s⁻¹ and the general appearance of the profiles is similar to that seen in OH 5.88-0.39 and OH 340.78-0.10, being suggestive of the emission from the front and back sides of an expanding (or contracting) shell. An H₂O maser with $v = +6$ km s⁻¹ coincides with the OH maser and both seem related to a quite compact HII region with mean velocity $+3$ km s⁻¹. This agreement with one peak of the OH emission (rather than the mean velocity of the two peaks) raises the possibility that the weaker OH emission between $+20$ and $+23$ km s⁻¹ represents ejecta from the principal source (which has a velocity near $+3$ km s⁻¹). Our position estimate of the $+20$ to $+23$ km s⁻¹ emission coincides (to within uncertainties of $\sim 40''$ arc) with the -2 to $+7$ km s⁻¹ emission and this makes it unlikely that it represents a totally unrelated source. It is also unlikely, in view of the apparent HII region association, that the OH maser represents emission from the circumstellar shell of a late-type star; furthermore, no satellite-line emission has been detected and the absence of strong 1612 MHz emission in particular argues against a late-type star identification.

OH 10.62-0.38 (Fig. 2). This maser was discovered more than a decade ago and the 1665 MHz emission has retained the same velocity structure but increased in intensity by 30% (see Caswell and Robinson 1974). The 1667 MHz emission is still similar to that measured by Yngvesson *et al.* (1975) in 1973 and shows right-hand circular (RHC) and left-hand circular (LHC) polarization separated by 1.3 km s⁻¹, probably due to Zeeman splitting in a magnetic field of 3.7 mG; a magnetic field, slightly smaller but in the same sense, is suggested by the somewhat more complex 1665 MHz profile. An accurate position for the OH maser has recently been obtained

Figs 1-12. Spectra of OH main-line masers. The continuous thick curve denotes the right-hand sense of circular polarization and the thin (dashed) curves denotes the left-hand sense. In all figures the intensity scale refers to one sense of polarization so that the total intensity is the sum (not the mean) of the intensities in each polarization. The velocity resolution is 0.14 km s⁻¹ (0.8 kHz). All observations were made in the period 8-13 February 1982.

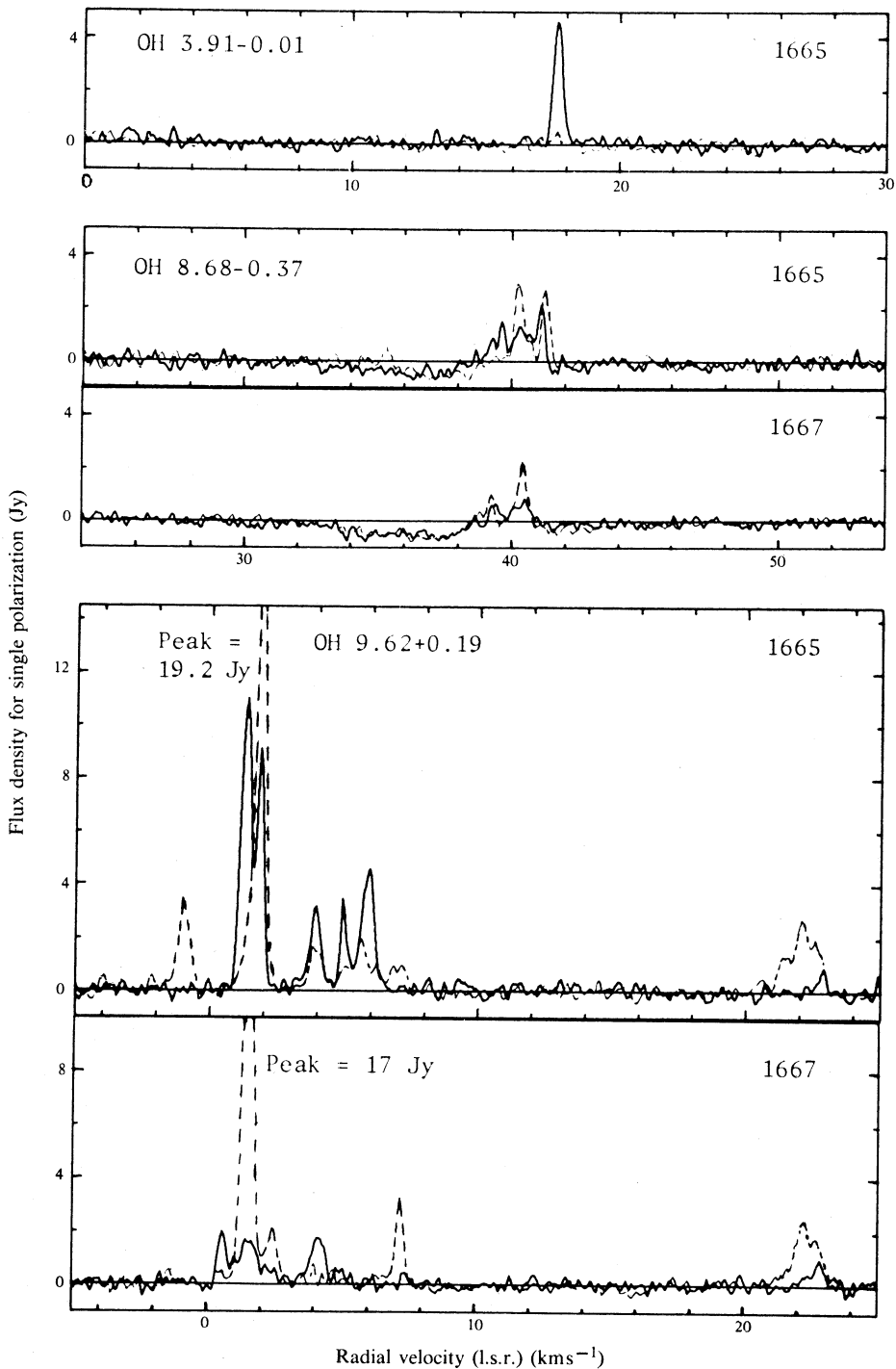


Fig. 1

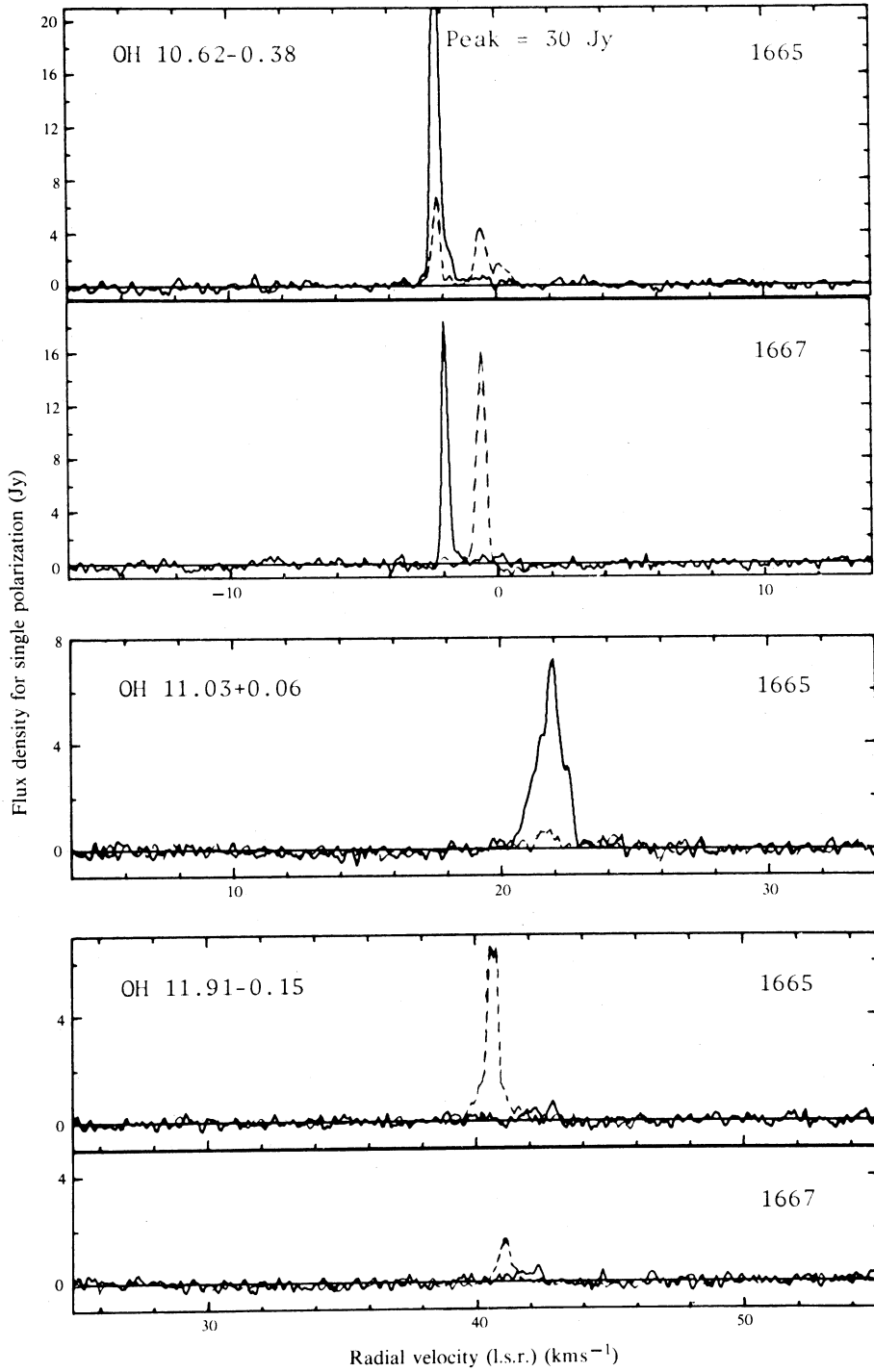


Fig. 2

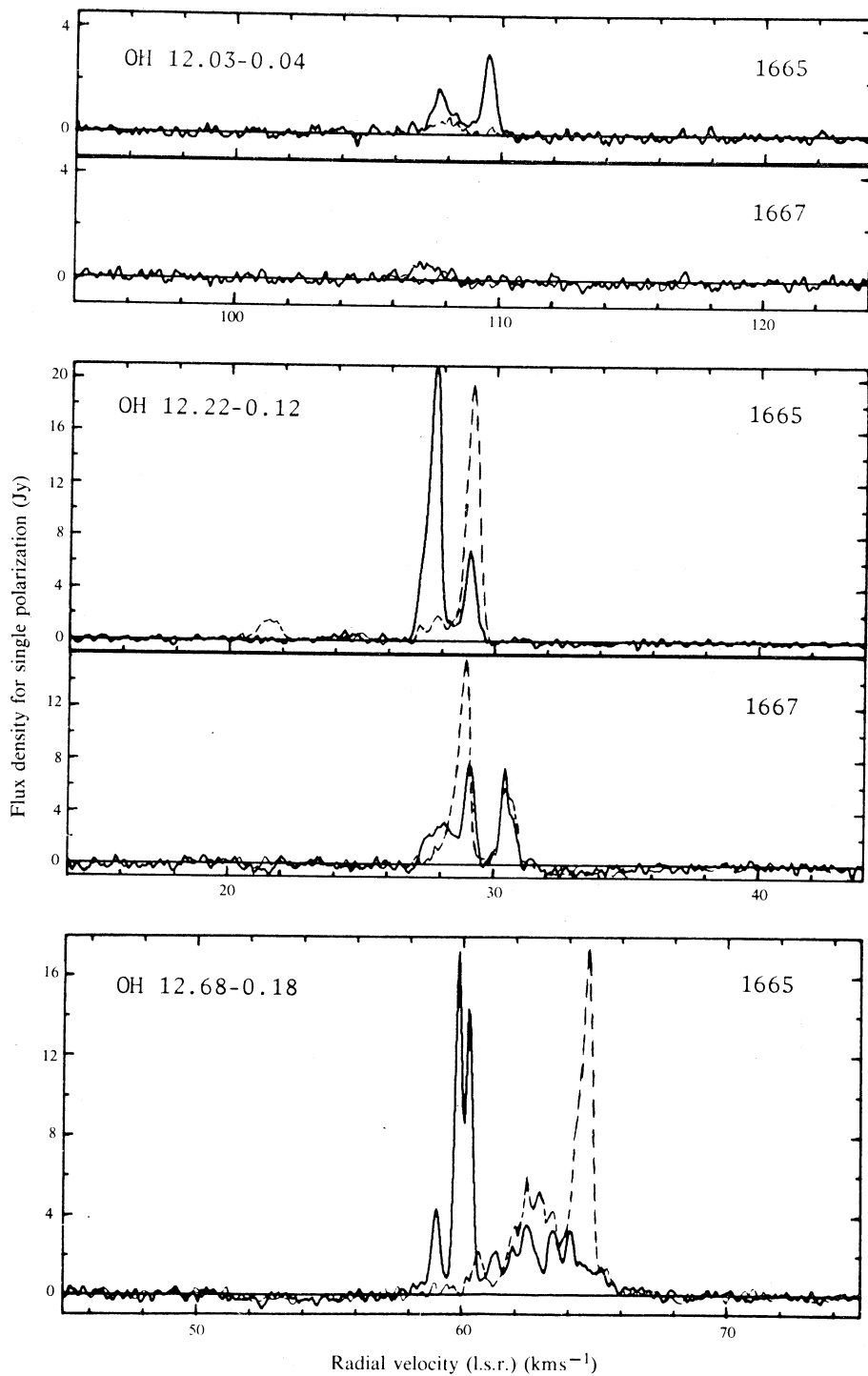


Fig. 3

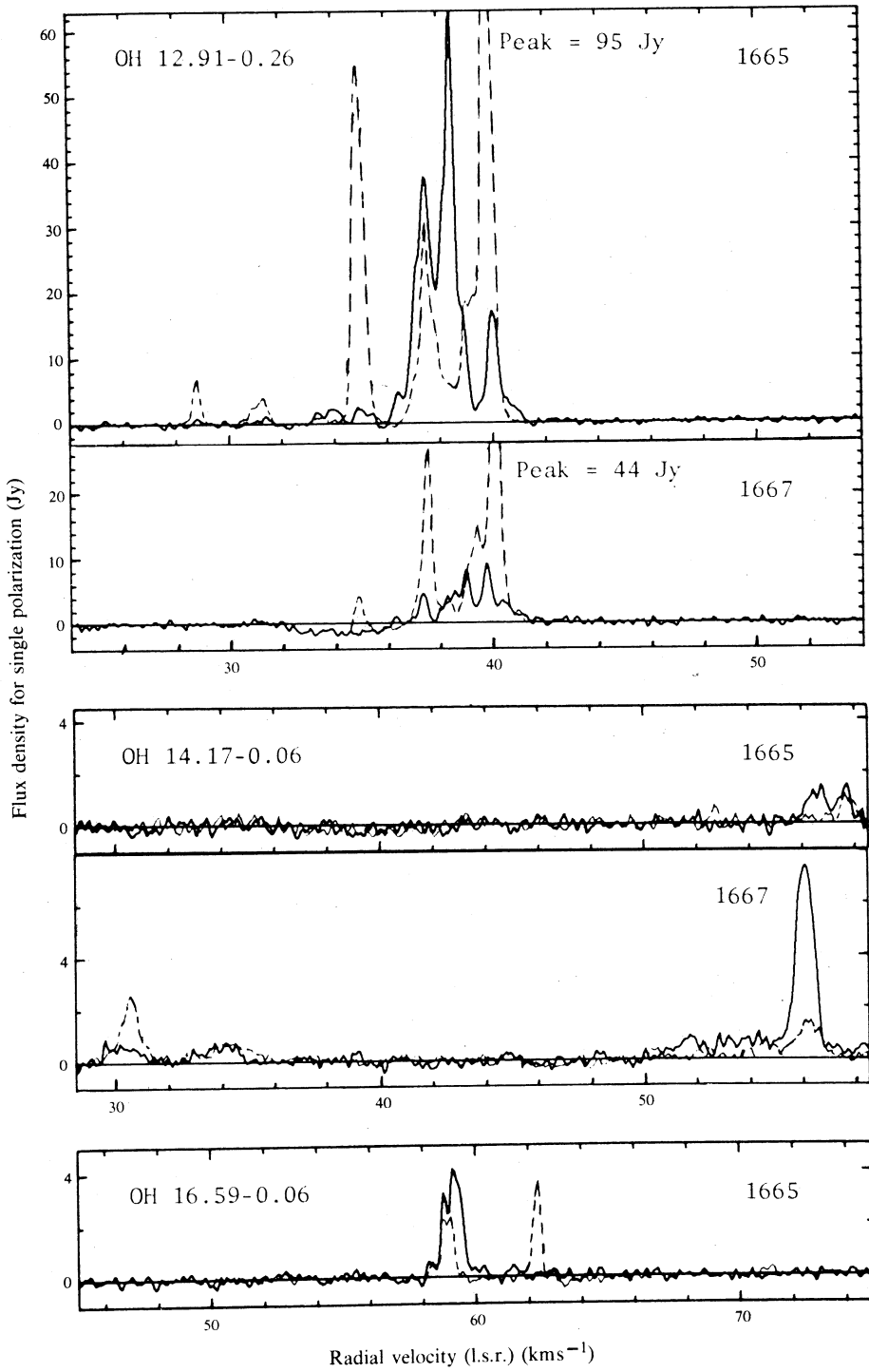


Fig. 4

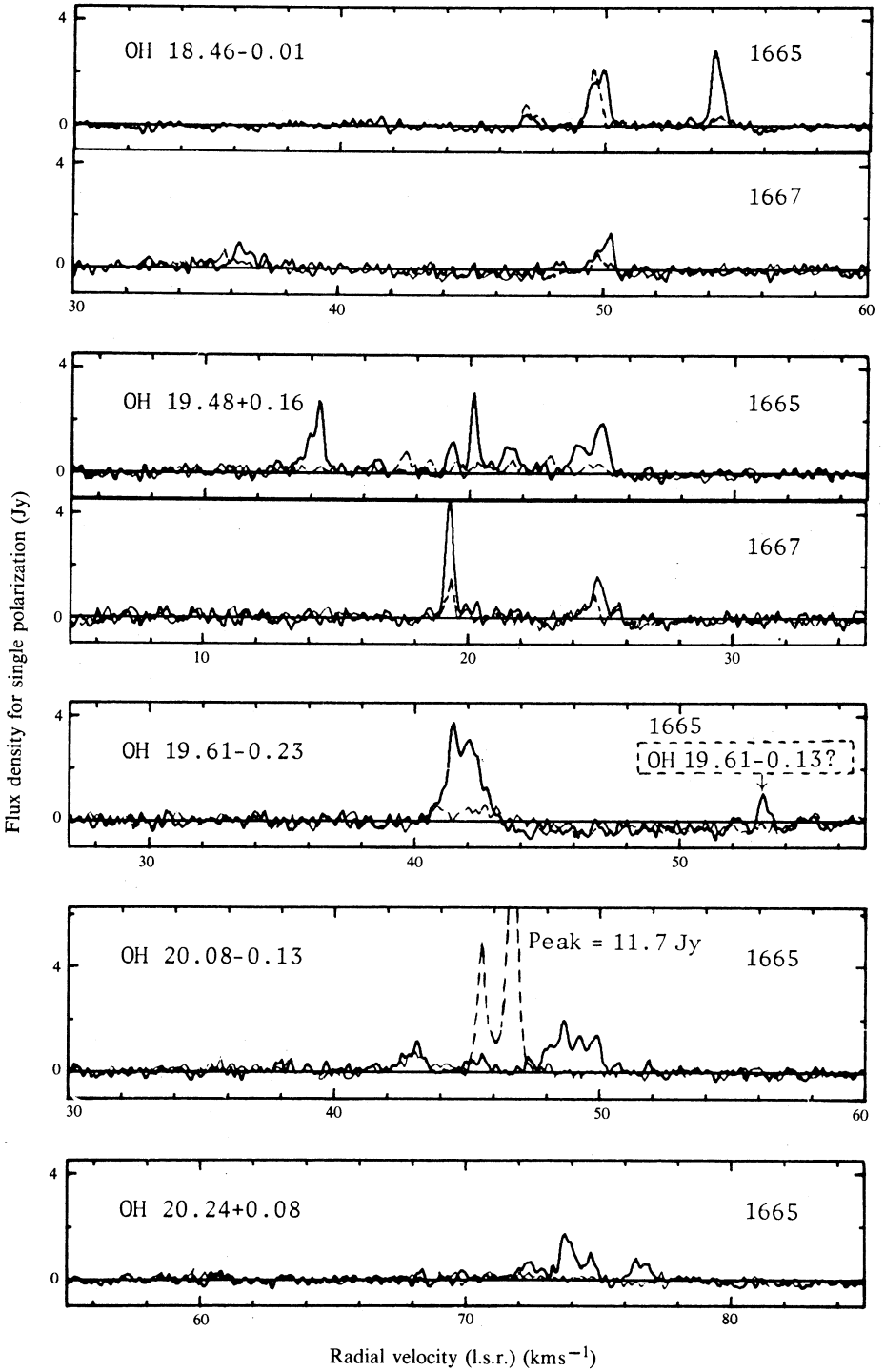


Fig. 5

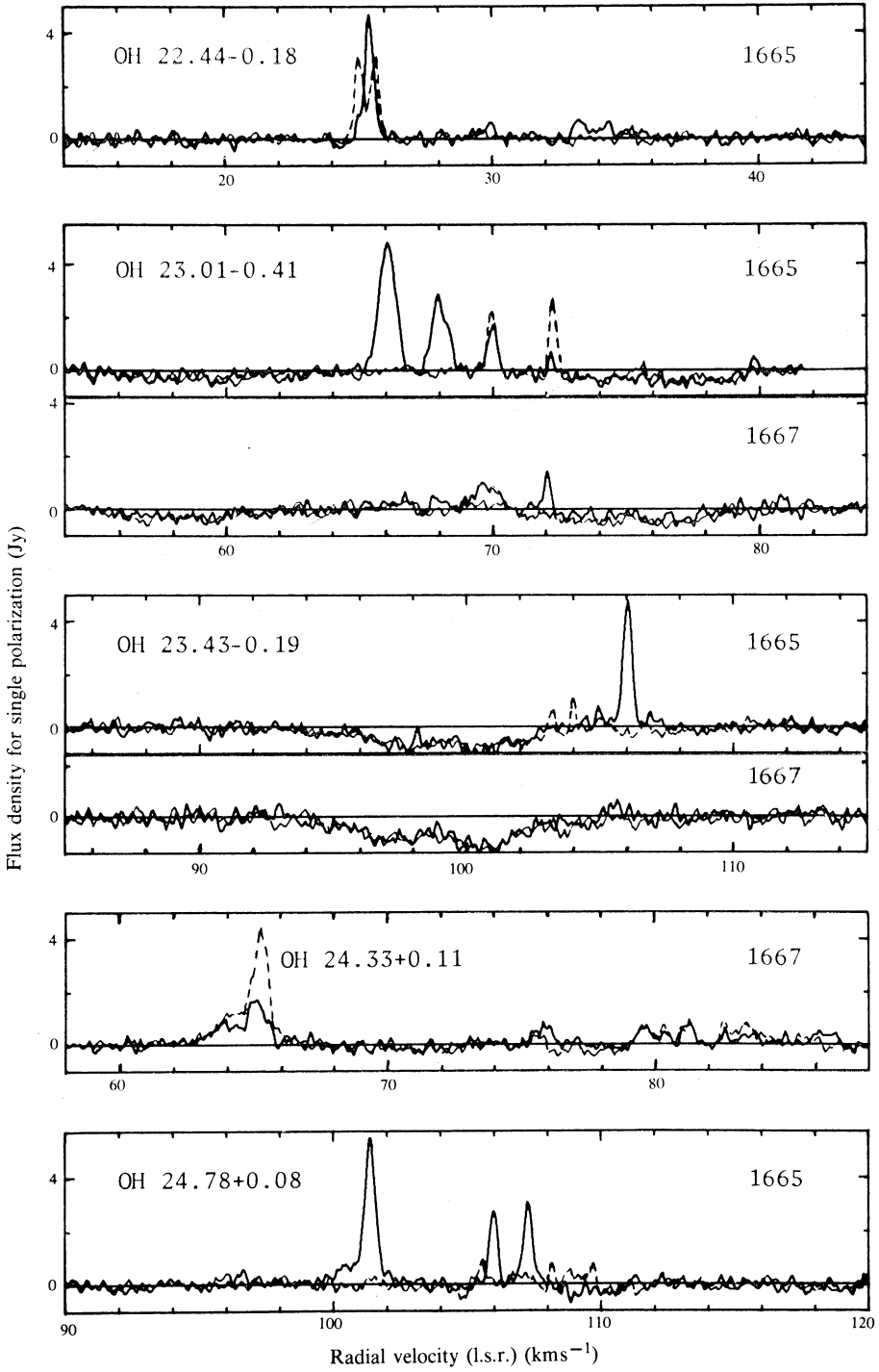


Fig. 6

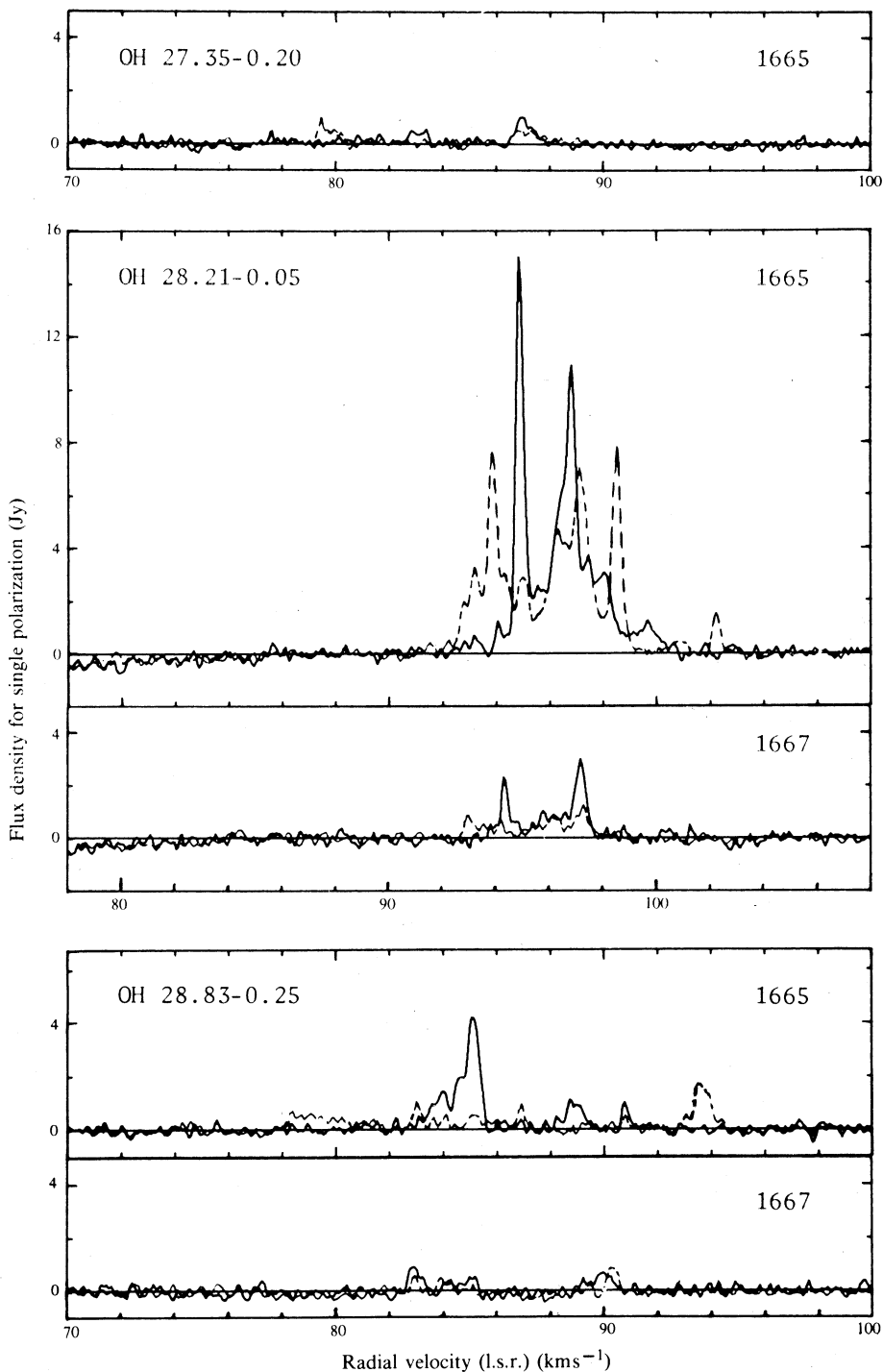


Fig. 7

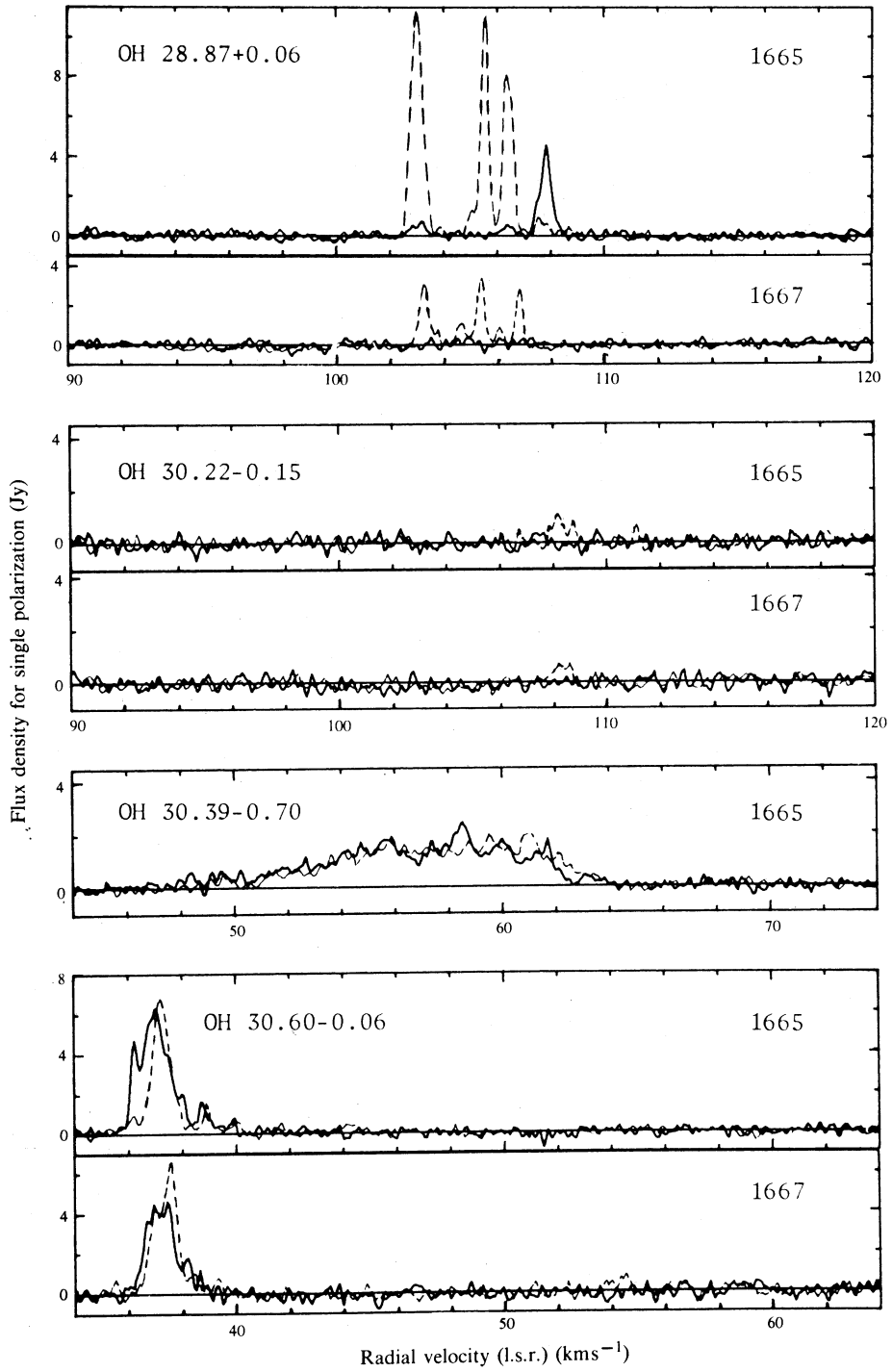


Fig. 8

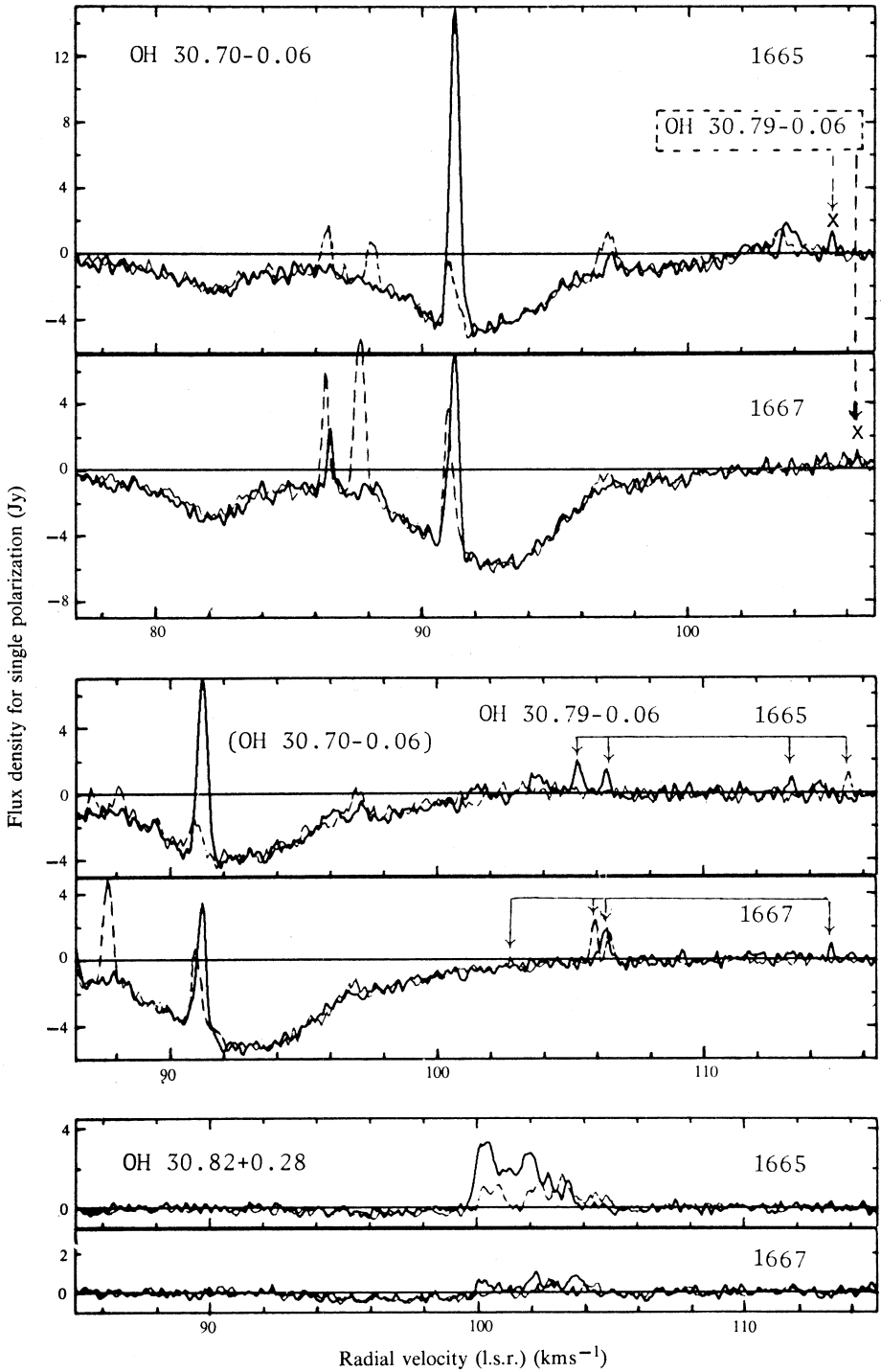


Fig. 9

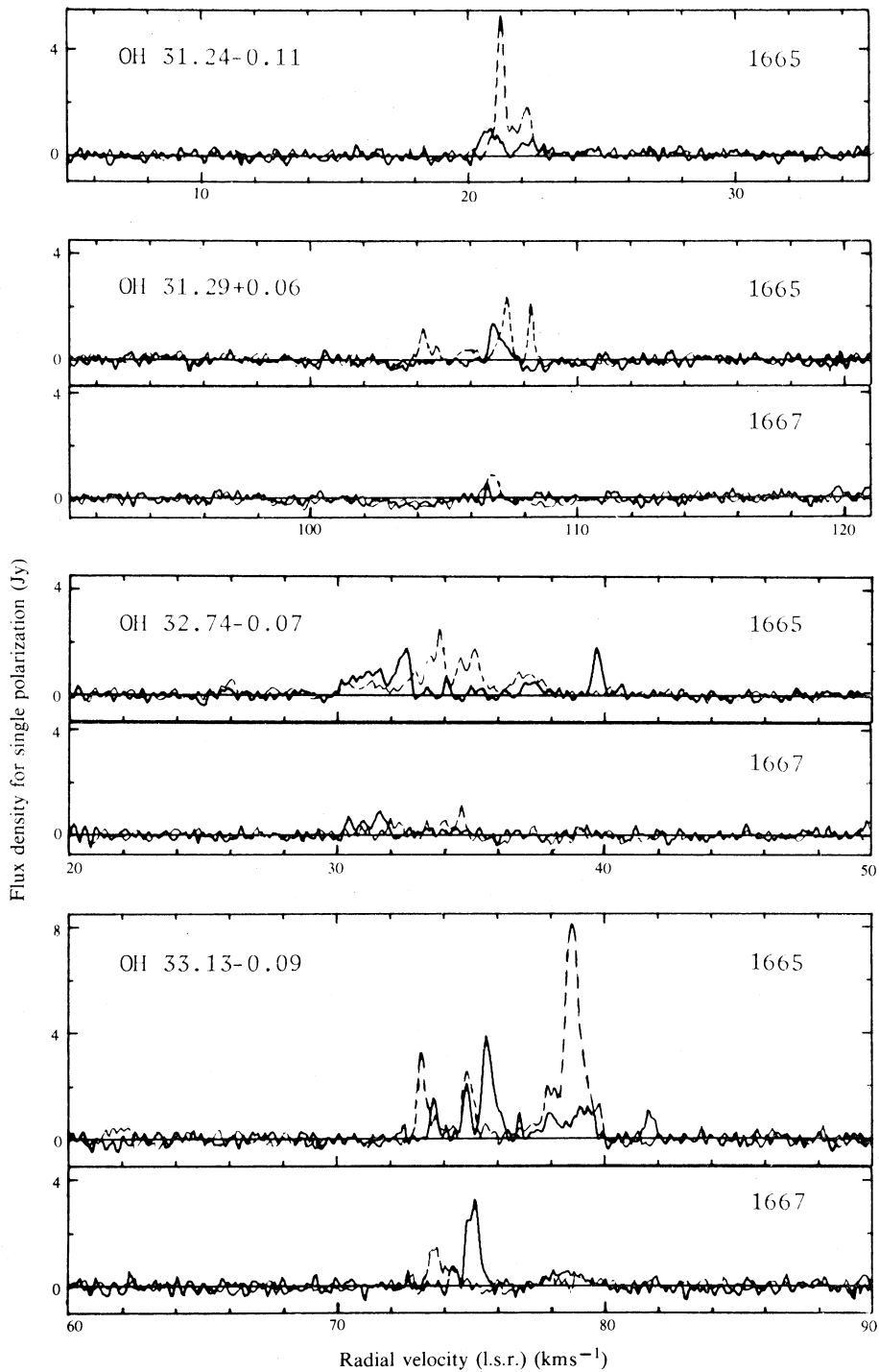


Fig. 10

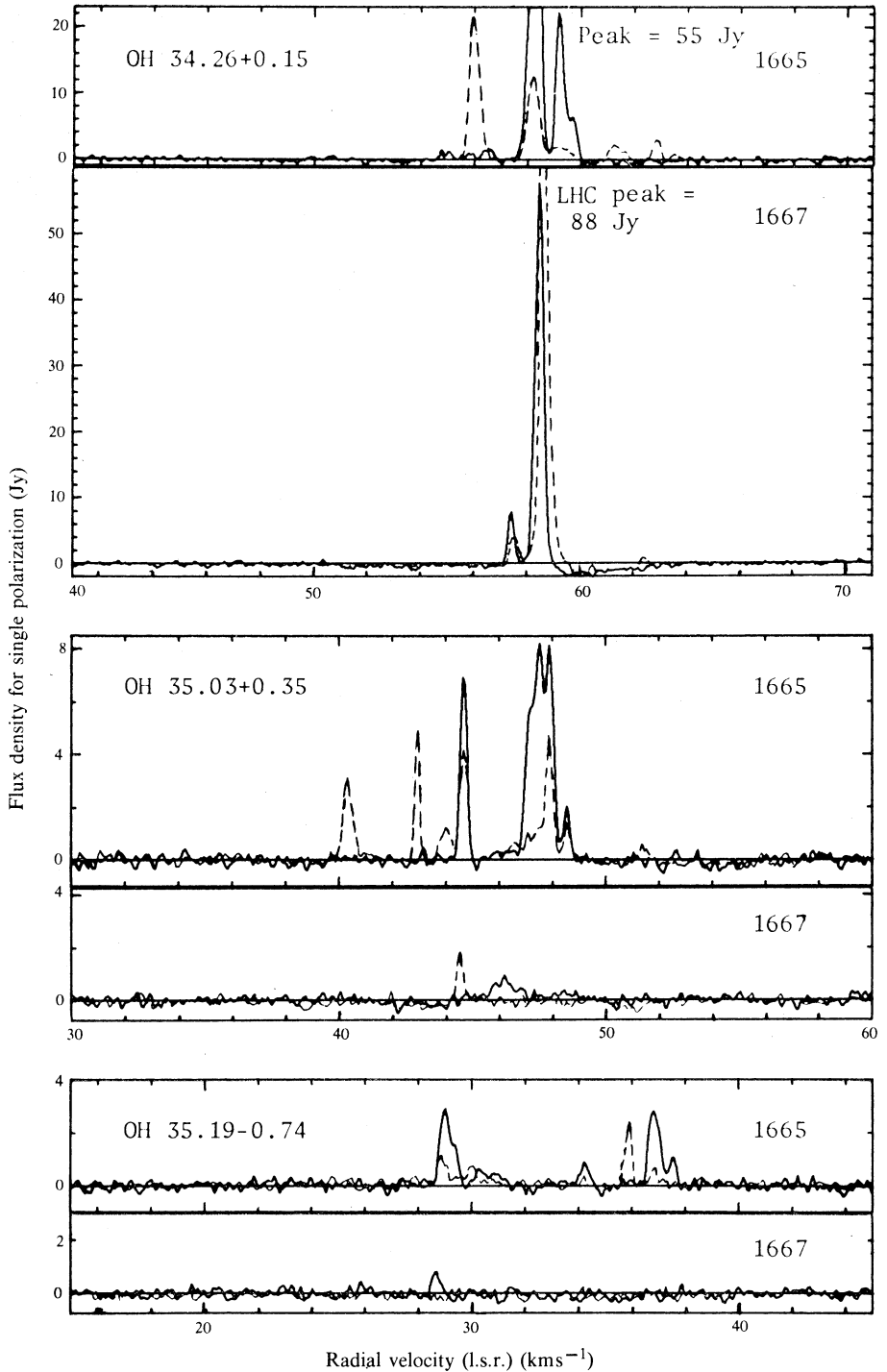


Fig. 11

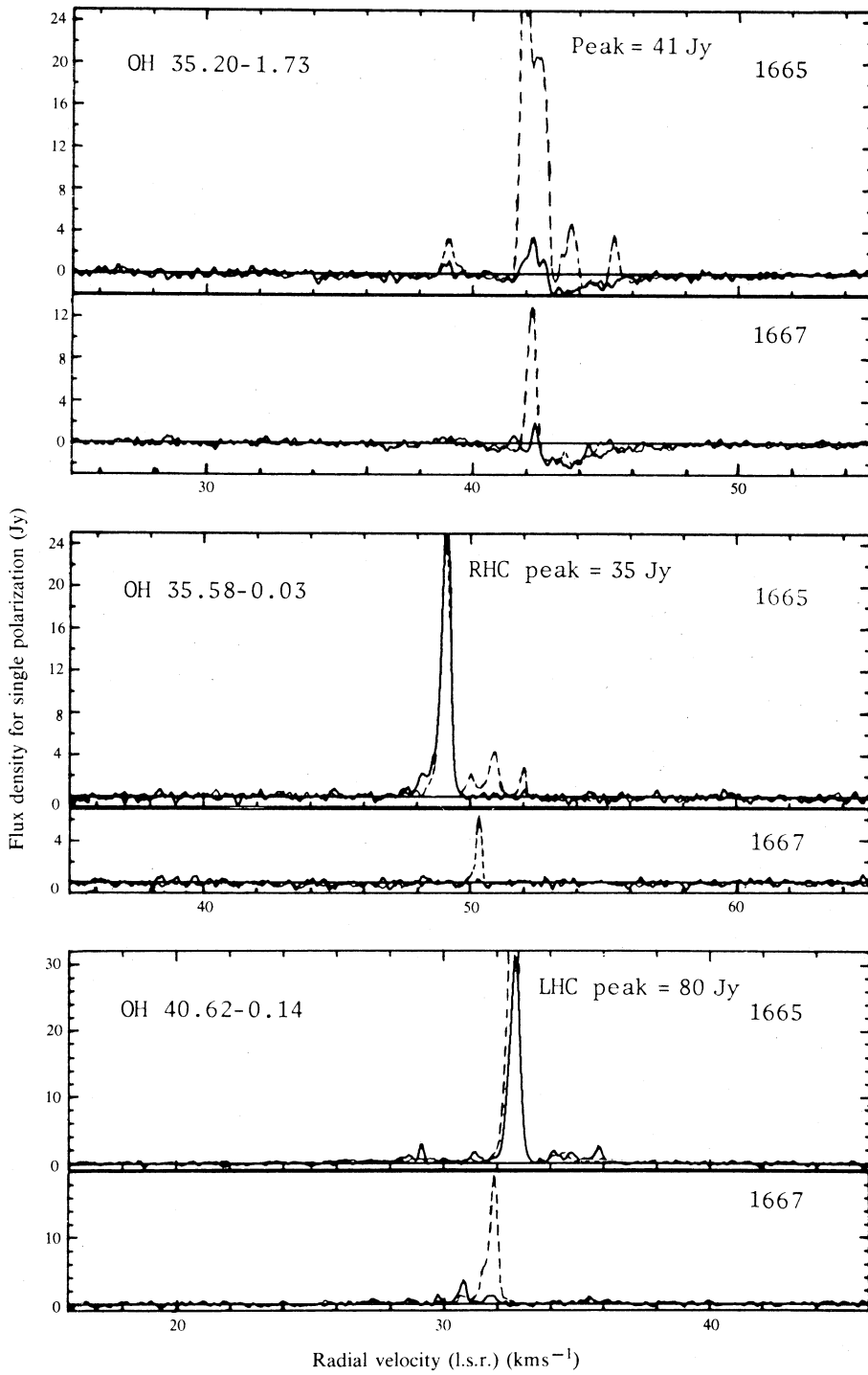


Fig. 12

by Turner (1982) (quoted in Table 1) and he finds good agreement, within several seconds of arc, with a compact (6" arc diameter) HII region. An H₂O maser is also present in this direction. The HII region complex may lie at a distance of ~ 6 kpc in the 3 kpc arm (Caswell *et al.* 1975b).

OH 11·03+0·06 (Fig. 2). The OH maser at 1665 MHz is a single feature, nearly 100% RHC polarized. Turner's (1979) data suggest that 1720 MHz emission is present but his failure to detect this with higher resolution observations (Turner 1982) suggests that it may be extended emission rather than a high-gain maser. An H₂O maser is present with $v = +11$ km s⁻¹ (displaced 10 km s⁻¹ from the OH peak) and a compact continuum source with flux density 0·4 Jy at 5 GHz is also present.

OH 11·91-0·15 (Fig. 2). OH maser emission is present at both 1665 and 1667 MHz and is predominantly LHC polarized. Although no strong compact continuum source is present the nearest HII region has a velocity similar to the OH emission, and this suggests that the OH maser is associated with the HII region complex.

OH 12·03-0·04 (Fig. 3). This is a new OH maser emitting at both 1665 and 1667 MHz with predominantly RHC polarization. The mean velocity of $+108$ km s⁻¹ is larger than any other maser or HII region at nearby longitudes; however, at a similar distance at the other side of the galactic centre ($l \approx 348^\circ$) there are sources with velocities of similar size but opposite sign; both these and OH 12·03-0·04 are presumably at the tangential point, at a distance of ~ 10 kpc.

OH 12·22-0·12 (Fig. 3). An HII region lies in the general direction of the OH maser and a weak (100 mJy at 1·7 GHz), more compact (1" arc) feature coincides with the OH maser (Turner 1982). Associated H₂O emission and IR data are discussed by Stier *et al.* (1982).

OH 12·68-0·18 (Fig. 3). This was one of the earliest OH maser discoveries (Goss 1968). The extensive HII emission in this general direction (W 33) shows recombination lines at both $+30$ and $+58$ km s⁻¹ and may represent either the superposition of two unrelated objects at different distances or a single object undergoing a massive disturbance (Gardner and Whiteoak 1972). A well-known H₂O maser coincides with the OH maser. Our current OH spectrum at 1665 MHz is generally similar to that of Robinson *et al.* (1970), but the $+59$ km s⁻¹ feature was nearly twice as strong 14 years ago, and the $+60$ km s⁻¹ feature, which is now very strong, was not detectable 14 years ago.

OH 12·91-0·26 (Fig. 4). This was discovered over a decade ago (Goss 1968). Strong LHC polarized emission near $v = +40$ km s⁻¹ is present at both 1665 and 1667 MHz and remains similar to its intensity 14 years ago (Robinson *et al.* 1970). The 1974 observations of Evans *et al.* (1979) at 1665 MHz show an intensity larger by nearly a factor of two, and from inspection of their data on other sources we suspect that all their intensities are too large by a factor of two—a common cause of confusion when converting antenna temperature to flux densities for highly polarized signals. In their Fig. 1 the labels of the LHC and RHC spectra are interchanged but their Table 2 is correct. Our current spectrum shows that the RHC emission at 1665 MHz near $v = +38$ km s⁻¹ is now much stronger than seen previously. An H₂O maser lies in this direction and a strong infrared source is present, but there is no compact radio continuum source (<5 mJy at 5 GHz) as reported by Jaffe *et al.* (1981).

OH 14.17-0.06 (Fig. 4). Currently the OH maser at 1667 MHz is stronger than at 1665 MHz and shows emission in two ranges of velocity, separated by 26 km s^{-1} . Our position measurements were made in 1975 when the 1667 MHz emission covered a similar velocity range but was weaker and showed little resemblance to the present spectrum. An H_2O maser (Batchelor *et al.* 1980) also shows emission over a similar range of velocity. There is complex continuum emission in the vicinity but no peak coincides with the maser position and the recombination-line velocity of $+31 \text{ km s}^{-1}$ is at one extreme of the maser velocity range.

OH 15.04-0.68. This is the only ground-state OH maser known in the large HII region M 17. No new observations have been made since our discovery measurement (Haynes *et al.* 1976); note that no position measurement has yet been made for the ground-state maser and that the position quoted is for the excited-state OH maser (Knowles *et al.* 1976). Several H_2O masers lie in the vicinity (Jaffe *et al.* 1981).

OH 16.59-0.06 (Fig. 4). Continuum maps show a source too weak (0.1 Jy) to permit recombination-line measurements.

OH 18.46-0.01 (Fig. 5). The 1665 MHz OH maser is accompanied by weaker emission at 1667 MHz, some of which is displaced about 10 km s^{-1} in velocity but is probably part of the same source, though our position measurements were made only at 1665 MHz. A weak (0.7 Jy) compact continuum source lies in this direction.

OH 19.48+0.16 (Fig. 5). Features are present at several velocities with comparable intensity at both 1665 and 1667 MHz. Weak 1612 MHz emission is seen on Turner's (1979) profile. The OH maser lies in the direction of an HII region which shows recombination-line emission at $+25 \text{ km s}^{-1}$ and is probably associated with the maser.

OH 19.61-0.23 (Fig. 5). The 1665 MHz emission is quite broad ($\sim 2 \text{ km s}^{-1}$) and is mainly RHC polarized. Its appearance is essentially unchanged from 1970 (Caswell and Robinson 1974). An HII region with $v = +43 \text{ km s}^{-1}$ lies in this direction and an H_2O maser, $\text{H}_2\text{O 19.61-0.23}$ (Genzel and Downes 1977), coincides with the OH maser. Our OH spectrum (Fig. 5) shows an additional weak feature with $v = +53 \text{ km s}^{-1}$; we have not positioned this feature but suspect that it is located $6'$ arc away near $l = 19.610$, $b = -0.133$, where there is another HII region (recombination-line velocity $+61 \text{ km s}^{-1}$) and another H_2O maser (with centre velocity $+50 \text{ km s}^{-1}$). If this is so the on-source intensity of this OH maser would be $\sim 2.5 \text{ Jy}$, twice the value seen on our spectrum.

OH 20.08-0.13 (Fig. 5). The 1665 MHz maser has changed very little in the past decade (cf. Caswell and Robinson 1974). A compact HII region (1.5 Jy , $v = +46 \text{ km s}^{-1}$) lies in the same direction.

OH 20.24+0.08 (Fig. 5). This weak 1665 MHz maser has no detectable continuum emission associated with it ($< 0.1 \text{ Jy}$).

OH 20.86+0.48. This unusual source has 1612 MHz emission approximately twice as strong as 1665 MHz emission and we have also detected weak 1667 MHz emission. Our 1665 MHz emission profile (not shown) shows no circular polarization. Winnberg *et al.* (1975) interpreted the maser as an atypical late-type star, but this remains uncertain.

OH 22.44-0.18 (Fig. 6). The nearest HII region is extended and has a velocity ($+78 \text{ km s}^{-1}$) quite different from that of the OH maser ($+26 \text{ km s}^{-1}$) and is presumably not associated with it.

OH 23·01–0·41 (Fig. 6). At both 1665 and 1667 MHz there is absorption from $v = +72$ to $+79$ km s⁻¹; this absorption, and the maser itself, are probably associated with the nearby diffuse HII emission at a velocity of $+78$ km s⁻¹. A second OH absorption feature at $v = +58$ km s⁻¹ may be at a different distance.

OH 23·43–0·19 (Fig. 6). The large velocity of this maser implies an unambiguous distance near the tangential point; an HII region is present at the same velocity.

OH 24·33+0·11 (Fig. 6). Despite the long period for which this maser has been known (Goss 1968), it remains a puzzle. Emission is detectable only at 1667 MHz. Goss *et al.* (1973) speculated that it might be an unusual OH/IR (late-type) star; recent measurements of recombination-line emission from nearby HII regions show them all to have velocities greater than 100 km s⁻¹, quite different from the OH maser, and lending support to the speculation of Goss *et al.* The spectrum now seen (Fig. 6) has changed markedly from 1969 (Robinson *et al.* 1970), and in the velocity range $+78$ to $+86$ km s⁻¹ the intensity has fallen by a factor of 10.

OH 24·78+0·08 (Fig. 6). Since our (unpublished) discovery observation in 1975, the feature at $v = +101·5$ km s⁻¹ has increased by a factor of three and the feature at $v = +107·5$ km s⁻¹ has decreased by a factor of three. Although the maser does not coincide with any continuum source several HII regions in the vicinity have velocities near 100 km s⁻¹, similar to the maser. An H₂O maser is associated with the OH maser.

OH 27·35–0·20 (Fig. 7). The OH maser lies near the edge of a diffuse HII region with velocity $+98$ km s⁻¹.

OH 28·21–0·05 (Fig. 7). At 1665 MHz the OH maser remains similar to our earlier (1975) measurement except that a feature now seen at $v = +95$ km s⁻¹ with peak intensity of 15 Jy was previously less than 4 Jy. Absorption is present near $v = +80$ km s⁻¹. A compact continuum source nearby is too weak (0·4 Jy) for a recombination-line measurement.

OH 28·83–0·25 (Fig. 7). The OH maser lies in the direction of a weak HII region with recombination-line velocity of $+92$ km s⁻¹.

OH 28·87+0·06 (Fig. 8). It is striking that both the 1665 and 1667 MHz masers are dominated by three narrow LHC polarized features, and at 1665 MHz there is, in addition, a RHC polarized feature. The continuum source in this direction is too weak to measure a recombination line. An associated H₂O maser has been found (Genzel and Downes 1979).

OH 30·22–0·15 (Fig. 8). This weak OH maser is seen mainly in LHC polarization at both 1665 and 1667 MHz. It lies in the direction of an HII region with $v = +101$ km s⁻¹. The OH position is poorly determined on account of its weakness (see column 4 in Table 1).

OH 30·39–0·70 (Fig. 8). Two considerations suggest that this maser may be associated with a late-type star: it is offset $0^{\circ}·7$ from the galactic plane, with no associated HII region and the 1612 MHz emission is stronger than the main lines. However, it differs from most late-type circumstellar masers in that the 1612 MHz emission shows a high degree of circular polarization (our unpublished data), while at 1665 MHz it appears almost unpolarized. The 1665 MHz emission is broad and has the characteristics of late-type stars with a steep fall-off in intensity at one extreme velocity but a gentler fall-off at the other velocity. Most OH/IR stars have emission

over two velocity ranges, and the 1665 MHz appearance would suggest a second peak at lower velocity but this has not been detected.

OH 30·60–0·06 (Fig. 8). This is one of the earliest maser discoveries (Goss 1968). The emission is of similar intensity at both 1665 and 1667 MHz and on both transitions the LHC polarized feature is shifted slightly to the high-velocity side of the RHC feature, suggestive of Zeeman splitting in a magnetic field of 0·5 mG. There has been remarkably little change in more than a decade (see Robinson *et al.* 1970). The spectrum of Fig. 8 does not extend much beyond the source on the low-velocity side; a separate 1665 MHz observation of the velocity range +18 to +34 km s⁻¹ showed no emission here. The maser lies in the direction of the strong W 43 continuum complex, which represents the superposition of two HII regions with velocities near 100 and 50 km s⁻¹.

OH 30·70–0·06 and 30·79–0·06 (Fig. 9). The two masers have similar velocities (near 100 km s⁻¹) and are approximately 6' arc apart, so that observations with our 12' arc beam centred on each source show the other source at half intensity. The masers lie close to the peak of the W 43 HII complex, which also has a similar velocity, near +100 km s⁻¹. The maser OH 30·79–0·06 shows several weak features, the 1667 MHz intensity being comparable with that of the 1665 MHz emission, while OH 30·70–0·06 is embedded in deep absorption and, again, shows several features at both 1665 and 1667 MHz.

Since our first observations of OH 30·79–0·06 (in 1975) at 1667 MHz a strong 6 Jy feature (RHC) at $v = +106$ km s⁻¹ has decreased in intensity and additional LHC emission is now present. The other source OH 30·70–0·06 shows all the same features as in 1975, but all somewhat stronger; in particular the RHC feature at 1665 MHz has increased by more than a factor of two. Three pairs of 1665 MHz features and two of 1667 MHz may indicate Zeeman splitting in a field of ~0·5 mG, all in the same sense, with the RHC feature at slightly more positive velocity than the LHC.

OH 30·82+0·28 (Fig. 9). The continuum map shows a weak source superimposed on very extended emission at the edge of the W 43 complex; the maser velocity is similar to that of the previous two sources.

OH 31·21–0·18. Although only a single peak in velocity is seen, this maser seems likely to be a late-type star because the 1612 MHz emission is larger, by a factor of five, than the 1665 MHz emission and the negative velocity probably indicates non-circular motions, which are much more common amongst late-type stars than in young-star-formation regions. The declination which we quote is for the 1612 MHz emission and is based on both our own measurements and those of Winnberg *et al.* (1981); note that the position derived by Evans *et al.* (1976) with an interferometer appears to have a two lobe-shift declination error of ~6' arc. A weak H₂O maser was detected at the correct OH position by Batchelor *et al.* (1980); Dickinson *et al.* (1978) claimed to have detected an H₂O maser 6' arc away at the incorrect declination of the OH position.

OH 31·24–0·11 (Fig. 10). The 1665 MHz OH maser is in an outlying portion of W 43, but its velocity, which differs markedly from either of the major HII region velocities, suggests it is unrelated to the main complex.

OH 31·29+0·06 (Fig. 10). The OH maser seems to be associated with an outlying compact feature in the W 43 complex and an H₂O maser has also been reported (Genzel and Downes 1979).

OH 32.74-0.07 (Fig. 10). The weak, diffuse, continuum emission in this direction has been interpreted as part of a supernova remnant, G 32.8-0.1, by Caswell *et al.* (1975a) and it seems unlikely to be closely related to the OH maser.

OH 33.13-0.09 (Fig. 10). At 1665 MHz the broad LHC polarized feature at $v = +79 \text{ km s}^{-1}$ has remained stable for the past decade (Caswell and Robinson 1974); a feature which was strong at $v = +74.5 \text{ km s}^{-1}$ in 1970 has fallen to less than a quarter of its earlier intensity. An HII region and an H₂O maser are associated.

OH 34.26+0.15 (Fig. 11). The 1665 MHz emission remains similar to our spectrum of more than a decade ago (unpublished data). Evans *et al.* (1979) tabulated intensities for 1974 which are twice as large but which we suspect are in error by a factor of two (see notes to OH 12.91-0.26). An H₂O maser and a strong HII region are associated.

OH 35.03+0.35 (Fig. 11). An associated continuum source is compact but too weak for a recombination-line measurement.

OH 35.19-0.74 (Fig. 11). Since 1976, our first observation at 1665 MHz, the feature at $v = +29 \text{ km s}^{-1}$ has decreased in intensity by a factor of two and new features have emerged near $+36$ and $+37 \text{ km s}^{-1}$. An H₂O maser is coincident (Batchelor *et al.* 1980) and there appears to be no closely associated continuum source; the nearest, which is compact and weak ($\sim 200 \text{ mJy}$), lies $\sim 3'$ arc south of the masers according to Altenhoff *et al.* (1978). A molecular cloud, recently detected by observations of strong NH₃ emission (Brown *et al.* 1982), envelops both the maser and continuum source, and has a mean velocity of 34 km s^{-1} .

OH 35.20-1.73 (Fig. 12). At both 1665 and 1667 MHz the major features seen in 1976 are still present but the 1665 MHz features at $+43.5$ and $+45 \text{ km s}^{-1}$ have now fallen in intensity by a factor of two. The OH masers are associated with an H₂O maser and a strong HII region.

OH 35.58-0.03 (Fig. 12). The 1665 MHz emission has changed very little since 1970 (Caswell and Robinson 1974). There is a strong HII region and an H₂O maser associated.

OH 40.62-0.14 (Fig. 12). With the assumption that the flux-density scale of Evans *et al.* (1979) is too large by a factor of two, we find little change between their 1974 observations and our 1982 spectrum. There is an associated H₂O maser but no detectable continuum source, with an upper limit of 15 mJy at both 2.7 and 8.1 GHz (Evans *et al.* 1979).

OH 43.16-0.03. Often referred to as W 49S; note that a 1720 MHz maser also occurs at this position.

OH 43.17+0.01. Often referred to as W 49N, the stronger of the two W 49 OH masers. Note that a 1612 MHz maser also occurs at this position. Recent high-sensitivity spectra were shown by Cohen and Willson (1981).

4. Discussion

Unusual Objects

In the previous section we mentioned a variety of unusual properties and here we summarize them. The sources OH 5.88-0.39, OH 9.62+0.19, OH 14.17-0.06 and OH 24.33+0.11 all show emission concentrated in two separated velocity ranges, which may indicate expanding (or contracting) shell structures. Sources which show

strong 1612 MHz emission are OH 5.88–0.39, OH 20.86+0.48, OH 30.39–0.70 and OH 31.21–0.18; this may suggest a late-type star identification, and for OH 31.21–0.18 the anomalous velocity seems to support this possibility.

Galactic Distribution of Sources

The OH sources tabulated do not represent a complete sample to a well-defined intensity limit and are not suitable for a detailed study of the galactic distribution. However, a comparison with the complementary range of galactic longitude south of the galactic centre (Caswell *et al.* 1980; Caswell and Haynes 1983) shows that approximately twice as many OH masers have been detected in the more systematic southern surveys. It would be valuable to extend the northern surveys to a similar level of completeness.

Polarization Properties

Relatively few sources show simple circular polarization and velocity structures indicative of Zeeman splitting; the only examples are OH 10.62–0.38, OH 30.60–0.06, OH 30.70–0.06 and OH 45.47+0.05. Several sources are highly polarized, either RHC or LHC, with the same sense of polarization predominant on both transitions; this may indicate large-scale gradients in velocity or magnetic field structures (Caswell *et al.* 1980).

Variability

For a satisfactory study of variability it is clearly desirable to compare data of high resolution (≤ 1 kHz) and with circular polarization information. For many sources the profiles published here are the only available data satisfying these requirements and it will require several years of monitoring to complete a variability study. However, for the sources known for several years there are many features which have remained stable for more than a decade, while a small fraction have shown dramatic variations (for example, changes by a factor of four) over several years.

Association with H₂O Masers

Approximately two-thirds of the masers of Table 1 are known to have an H₂O maser in the same general direction. We study this association in the light of new H₂O data in a further paper (Caswell *et al.* 1983, present issue p. 443).

5. Update to Source List

Little and Cesarsky (1982) listed several new OH masers, one of which, OH 31.40+0.30, is strong enough to be included in the Table 1 list of sources greater than 1 Jy intensity. With a frequency resolution of 6 kHz, Little and Cesarsky found peak intensities of ~ 6 Jy at 1667 MHz, ~ 1.3 Jy at 1665 MHz and ~ 4.4 Jy at 1720 MHz, the velocity of emission lying between +97 and +104 km s⁻¹.

In our discussion of OH 19.61–0.23 we referred to another maser, OH 19.61–0.13, which is probably $\sim 6'$ arc away; this too should be added to the list of OH masers when its position has been accurately determined.

6. Conclusions

The present atlas of OH masers provides a homogeneous set of OH data, and it will now be necessary to complement this with more complete data on possible associated objects: in particular, weak compact HII regions (requiring sensitive high-resolution observations), infrared measurements, and H₂O maser measurements. Precise relative position measurements will be necessary to understand fully what conditions are vital to the spontaneous formation of the celestial masers.

References

- Altenhoff, W. J., Downes, D., Pauls, T., and Schraml, J. (1978). *Astron. Astrophys. Suppl.* **35**, 23.
- Batchelor, R. A., Caswell, J. L., Goss, W. M., Haynes, R. F., Knowles, S. H., and Wellington, K. J. (1980). *Aust. J. Phys.* **33**, 139.
- Baud, B., Habing, H. J., Matthews, H. E., and Winnberg, A. (1979). *Astron. Astrophys. Suppl.* **35**, 179.
- Brown, A. T., Little, L. T., MacDonald, G. H., and Matheson, D. N. (1982). *Mon. Not. R. Astron. Soc.* **201**, 121.
- Caswell, J. L., Batchelor, R. A., Forster, J. R., and Wellington, K. J. (1983). *Aust. J. Phys.* **36**, 443.
- Caswell, J. L., Clark, D. H., and Crawford, D. F. (1975a). *Aust. J. Phys. Astrophys. Suppl.* No. 37, 39.
- Caswell, J. L., and Haynes, R. F. (1975). *Mon. Not. R. Astron. Soc.* **173**, 649.
- Caswell, J. L., and Haynes, R. F. (1983). *Aust. J. Phys.* **36**, 361.
- Caswell, J. L., Haynes, R. F., and Goss, W. M. (1980). *Aust. J. Phys.* **33**, 639.
- Caswell, J. L., and Robinson, B. J. (1974). *Aust. J. Phys.* **27**, 597.
- Caswell, J. L., Roger, R. S., Murray, J. D., Cole, D. J., and Cooke, D. J. (1975b). *Astron. Astrophys.* **45**, 239.
- Cohen, N. L., and Willson, R. F. (1981). *Astron. Astrophys.* **96**, 230.
- Dickinson, D. F., Blair, G. N., Davis, J. H., and Cohen, N. L. (1978). *Astron. J.* **83**, 32.
- Downes, D., Wilson, T. L., Bieging, J., and Wink, J. (1980). *Astron. Astrophys. Suppl.* **40**, 379.
- Epchtein, N., and Rieu, N.-Q. (1982). *Astron. Astrophys.* **107**, 229.
- Evans, N. J., Beckwith, S., Brown, R. L., and Gilmore, W. (1979). *Astrophys. J.* **227**, 450.
- Evans, N. J., Crutcher, R. M., and Wilson, W. J. (1976). *Astrophys. J.* **206**, 440.
- Gardner, F. F., and Whiteoak, J. B. (1972). *Astrophys. Lett.* **12**, 107.
- Genzel, R., and Downes, D. (1977). *Astron. Astrophys. Suppl.* **30**, 145.
- Genzel, R., and Downes, D. (1979). *Astron. Astrophys.* **72**, 234.
- Goss, W. M. (1968). *Astrophys. J. Suppl. Ser.* **15**, 131.
- Goss, W. M., Lockhart, I. A., Formalont, E. B., and Hardebeck, E. G. (1973). *Astrophys. J.* **183**, 843.
- Hardebeck, E. G. (1972). *Astrophys. J.* **172**, 583.
- Haynes, R. F., Caswell, J. L., and Goss, W. M. (1976). *Proc. Astron. Soc. Aust.* **3**, 57.
- Haynes, R. F., Caswell, J. L., and Simons, L. W. J. (1978). *Aust. J. Phys. Astrophys. Suppl.* No. 45, 1.
- Jaffe, D. T., Güsten, R., and Downes, D. (1981). *Astrophys. J.* **250**, 621.
- Jones, T. J., Hyland, A. R., and Gatley, I. (1983). *Astrophys. J.* (in press).
- Knowles, S. H., Caswell, J. L., and Goss, W. M. (1976). *Mon. Not. R. Astron. Soc.* **175**, 537.
- Little, L. T., and Cesarsky, D. A. (1982). *Astron. Astrophys.* **112**, 49.
- Norris, R. P., Booth, R. S., Diamond, P. J., and Porter, N. D. (1982). *Mon. Not. R. Astron. Soc.* **201**, 191.
- Raimond, E., and Eliasson, B. (1969). *Astrophys. J.* **155**, 817.
- Robinson, B. J., Goss, W. M., and Manchester, R. N. (1970). *Aust. J. Phys.* **23**, 363.
- Schmidt, M. (1965). In 'Galactic Structure' (Eds A. Blaauw and M. Schmidt), p. 513 (Univ. Chicago Press).
- Stier, M. T., Jaffe, D. T., Fazio, G. G., Roberge, W. G., Thum, C., and Wilson, T. L. (1982). *Astrophys. J. Suppl.* **48**, 127.
- ter Meulen, J. J., and Dymanus, A. (1972). *Astrophys. Lett.* **172**, L21.
- Turner, B. E. (1969). *Astrophys. J.* **157**, 106.
- Turner, B. E. (1979). *Astron. Astrophys. Suppl.* **37**, 1.
- Turner, B. E. (1982). In 'Regions of Recent Star Formation' (Eds R. S. Roger and P. E. Dewdney), p. 425 (Reidel: Dordrecht).

- Winnberg, A., Nguyen-Q-Rieu, Johansson, L. E. B., and Goss, W. M. (1975). *Astron. Astrophys.* **38**, 145.
- Winnberg, A., Terzides, Ch., and Matthews, H. E. (1981). *Astron. J.* **86**, 410.
- Wynn-Williams, C. G., Werner, M. W., and Wilson, W. J. (1974). *Astrophys. J.* **187**, 41.
- Yngvesson, K. S., Cardiasmos, A. G., Shanley, J. F., and Rydbeck, O. E. H. (1975). *Astrophys. J.* **195**, 91.

Manuscript received 18 November, accepted 9 December 1982